LASER diode-based transmitter module for optical wireless communications

João H. Araújo[1,2], Rafael Kraemer[1], H. M. Santos[1,3], Francisco Pereira[2], H. M. Salgado[1,3], and L. M. Pessoa[1,3]
[1]*INESC TEC - Institute for Systems and Computer Engineering, Technology and Science, Porto, Portugal*
[2]*School of Engineering, Polytechnic Institute of Porto, Porto, Portugal*
[3]*Faculty of Engineering, University of Porto, Porto, Portugal*
e-mail: {joao.h.araujo, rafael.kraemer, hugo.m.santos, henrique.salgado, luis.m.pessoa}@inesctec.pt, fdp@isep.ipp.pt

***Abstract*—In this paper, we present the design of an analog transmitter based on a blue LD targeting optical wireless communications, suitable for OFDM signals. The approach relies on a thorough characterization of the individual components of the module, whence a detailed circuit model is obtained to design an impedance matching circuit for improved performance, prior to fabrication. The impedance matching is based on non-uniform transmission lines and works well over a wide frequency range (100 MHz to 2 GHz). The results are experimentally validated by the transmitter response exhibiting an increased 6 dB bandwidth limit and 1 GHz bandwidth improvement.**

***Index Terms*—Optical wireless communications transmitter, SOLT calibration kit, bias-tee, impedance matching circuit.**

I. Introduction

In recent years, optical wireless communications have been attracting much interest, whether free-space or underwater. Free-space optical communications involve the transmission of optical beams through the atmosphere in order to establish broadband communications. They are essentially motivated by the scarcity of the RF spectrum and the increase in transmission requirements, such as high bandwidth, high robustness, low transmission errors, low cost, high portability, and security. Underwater optical communications have also been widely targeted especially by coastal countries. This interest is essentially motivated by the fact that existing natural resources are increasingly scarce, and countries need to ensure access to and use of underwater natural resources [1].

In the context of optical wireless communications (OWC), the use of a LASER diode (LD) in the transmission systems is widely employed. When compared to light-emitting diodes, LDs provide higher output optical power, allow for a higher modulation bandwidth and subsequently a higher transmission bandwidth, therefore being an appropriate choice for high throughput optical wireless communications [2]. However, these light sources have a large temperature dependency, with additional control circuits typically being required, such as those based on thermoelectric coolers (TECs). Here we discuss the design of an analog LD based optical transmitter, adequate for the transmission of radiofrequency (RF) signals such as orthogonal-frequency division multiplexing (OFDM). In this instance, the transmitter, depicted in Fig. 1, is composed of a bias-tee for coupling the signal and bias to the LD provided by a current source and a temperature control circuit.

This work is financed by the ERDF – European Regional Development Fund through the Operational Programme for Competitiveness and Internationalisation - COMPETE 2020 Programme and by National Funds through the Portuguese funding agency, FCT - Fundação para a Ciência e a Tecnologia within project POCI-01-0145-FEDER-031971.

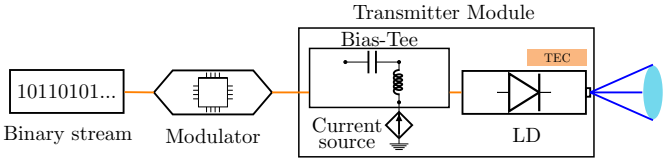

Fig. 1. Block diagram of an LD based OWCs transmitter.

The design of the optical transmitter on computer-aided design software would be inaccurate if proper modeling of the impedance mismatch between the LD and the driver circuit, including the bias-tee, is not accounted for. Hence, the need to characterize the individual components accurately, which usually requires the use of a vector network analyzer (VNA), with subsequent inclusion of these models into the simulation environment. This approach is addressed and described in this paper, to properly design the matching circuit of such a transmitter system to model accurately the performance of the system prior to fabrication. The complete system is further validated experimentally.

For the experimental characterization of each component printed circuit board (PCB) test fixtures were specifically designed and manufactured to this purpose, as well as a calibration kit that reproduces its physical and electrical properties. This is required since the VNA needs to know a priori the measurement conditions in order to be able to subtract the board's inherent effects, namely the existence of possible interferences, mismatches or parasitic capacitances, the effect introduced by the connectors, as well as the transmission lines. This process is known as de-embedding [3].

The remainder of this paper is organized as follows: Section II presents the design of the calibration kit and the configuration of the measurement equipment; the design of the bias-tee and a discussion of its performance is described in Section III; Section IV addresses the characterization of LD performance and the design of the impedance matching circuit and it affects the frequency response of the system; in Section V the whole transmitter module is detailed; in Section VI the experimental

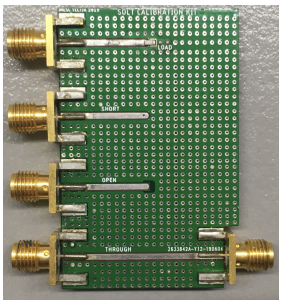

(a) Calibration kit.

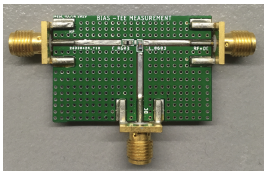

(b) Bias-tee test fixture.

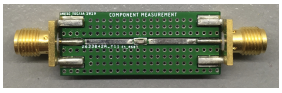

(c) Component test fixture.

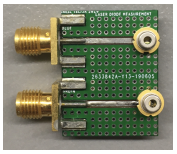

(d) LDs test fixture.

Fig. 2. Designed PCBs.

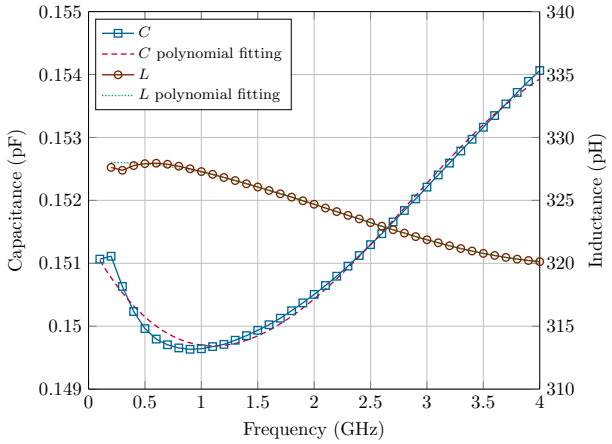

Fig. 3. Inductance and capacitance as functions of the frequency and their polynomial approximations.

results are presented and discussed; the final conclusions are given in Section VII.

II. Calibration Kit

In fact, there are several approaches to design a calibration kit such as short-open-load-through (SOLT), through-reflect-line (TRL), line-reflect-match (LRM), line-reflect-reflect-match (LRRM), among others [3]. The SOLT method was used in this work since the other mentioned calibration methods would require very long line standards (typically $\lambda/4$), as the minimum measurement frequency was $100\,\mathrm{MHz}$. Additionally, a maximum operation bandwidth of $4\,\mathrm{GHz}$ was considered.

The configuration of the selected transmission line for the implementation of the test fixture PCBs was based on a conductor-backed coplanar waveguide (CBCPW), which was previously optimized for a characteristic impedance of $Z_0 = 50\,\Omega$ [4]. The transmission line was designed with a trace width of $1.1\,\mathrm{mm}$ and considering an FR-4 dielectric substrate with a thickness of $0.8\,\mathrm{mm}$ and a relative permittivity of 4.6. SMA $50\,\Omega$ gold plated edge mount connectors were used for coupling. Fig. 2 shows the designed calibration kit and the test fixture PCBs used to measure the bias-tee components, bias-tee circuit, and two different LDs.

Having designed the calibration kit, the actual measurement requires the configuration of the VNA with the de-embedding parameters. These in turn are constituted by eight coefficients that result from a polynomial representation of the inductance and capacitance of the PCB test fixtures, as functions of frequency. The coefficients of the inductance and capacitance were extracted numerically, through 3D electromagnetic simulations, from the short and open circuit elements, respectively. The simulation made use of detailed 3D models of the test fixtures and was based on the method of moments, from which the reflection coefficients (S_{11}) were obtained. With this parameter, it was possible to obtain the load impedance (Z_l) of each one-port network element, as described by (1) [5].

TABLE I
Obtained coefficients from the polynomial approximations of the inductance and capacitance.

Inductance	Capacitance
$L_0 = 327.95 \times 10^{-12}\,\mathrm{H}$	$C_0 = 151.36 \times 10^{-15}\,\mathrm{F}$
$L_1 = 656.98 \times 10^{-24}\,\mathrm{H/Hz}$	$C_1 = -3286.10 \times 10^{-27}\,\mathrm{F/Hz}$
$L_2 = -1626.30 \times 10^{-33}\,\mathrm{H/Hz^2}$	$C_2 = 1841.90 \times 10^{-36}\,\mathrm{F/Hz^2}$
$L_3 = 243.82 \times 10^{-42}\,\mathrm{H/Hz^3}$	$C_3 = -214.94 \times 10^{-45}\,\mathrm{F/Hz^3}$

$$Z_l = \frac{Z_0\,(1 + S_{11})}{1 - S_{11}} \tag{1}$$

The inductance (L) and the capacitance (C) as functions of the frequency (f) are given, respectively, by (2) and (3), where $\mathrm{Im}\{Z_l\}$ represents the imaginary part of Z_l. Fig. 3 shows its frequency dependence, as well as its polynomial approximations.

$$L = \frac{\mathrm{Im}\{Z_l\}}{2\pi f} \tag{2}$$

$$C = \frac{-1}{\mathrm{Im}\{Z_l\} 2\pi f} \tag{3}$$

In Table I, we present the obtained coefficients from the polynomial approximation of the inductance and the capacitance as functions of the frequency that allowed a correct configuration of the calibration kit in the VNA.

III. Bias-Tee

The most important parameters to evaluate the performance of a bias-tee circuit, represented in Fig. 4, are the reflection and transmission coefficients and the isolation from the RF port to the DC port, which are obtained through the analysis of the scattering parameters (S-parameters) of the circuit.

In order to obtain the capacitor and inductor values, an exhaustive study was performed, in which several components from three different manufacturers were experimentally evaluated. After analyzing the reflection and transmission coefficients and the bandwidth of each component using the designed

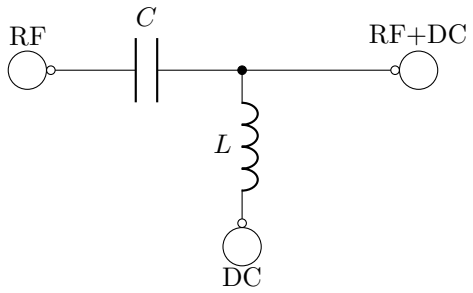

Fig. 4. Configuration of the bias-tee circuit.

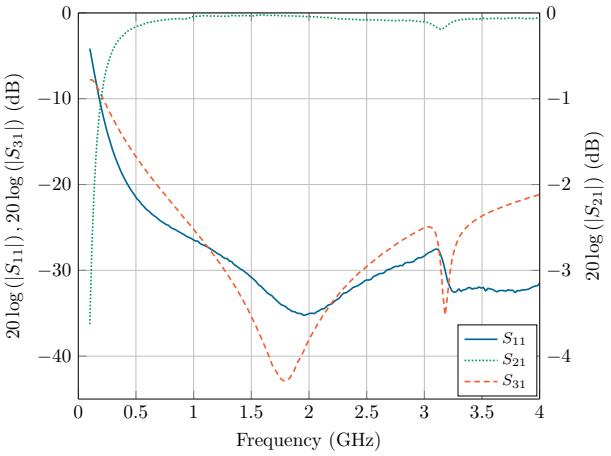

Fig. 5. Reflection and transmission coefficients and isolation of the bias-tee.

PCB test fixture shown in Fig. 2c, the result that maximizes the three metrics was obtained for a capacitor of 22 pF (AVX 06033J220FBSTR) and an inductor of 100 nH (Coilcraft 0603CS-R10). Thus, the circuit characteristics were measured in the already de-embedded VNA, through the designed PCB test fixture shown in Fig. 2b.

The measured reflection (S_{11}) and transmission (S_{21}) coefficients, and the isolation (S_{31}) from the bias-tee circuit, are shown in Fig. 5. It can be verified that the reflection coefficient, which should be as low as possible to minimize the return signal at the circuit input, is less than -25 dB from 800 MHz and less than -30 dB from 1.45 GHz to around 2.7 GHz. The transmission coefficient, which should be close to 0 dB to minimize the signal loss in the circuit, is less than -0.2 dB from 500 MHz with a very low ripple. The isolation, which should be as low as possible to minimize the RF signal at the DC terminal, is higher than 20 dB from 700 MHz and higher than 30 dB from 1.30 GHz to 2.45 GHz.

IV. Laser Diode Matching Circuit

According to [6], water shows a lower absorption coefficient on the wavelengths between 400 nm - 600 nm, which corresponds to the blue and green spectrum. For this reason, in this work, the transmitter was designed for operation with a 450 nm (blue) InGaN LD. LDs have an intrinsic maximum operation bandwidth within tenths of GHz range, determined

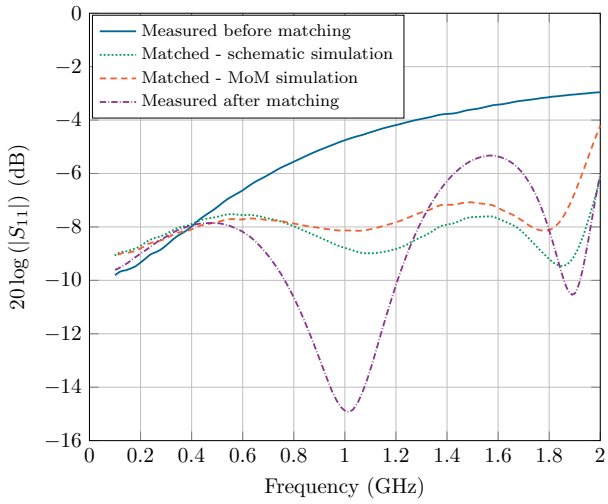

Fig. 6. Measured reflection coefficient of the LD and simulated improvement with the introduction of the impedance matching circuit.

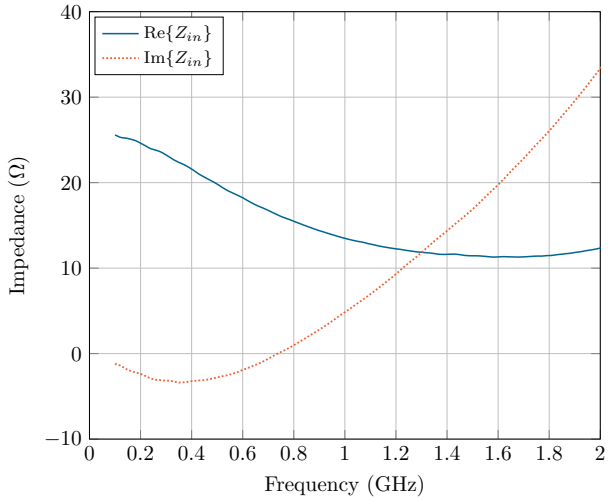

Fig. 7. Input impedance of the LD.

by the differential gain, gain compression and ultimately carrier lifetime [7], [8]. However, the package and chip parasitics may further limit the operating frequency to a few GHz, which is the case of the diode PLT5-450B by Osram used in this work. As such the transmitter performance was evaluated from 100 MHz to 2 GHz.

The reflection coefficient and the impedance of the LD were measured through the previously presented PCB test fixtures from Fig. 2d. The measured reflection coefficient of the LD is shown in Fig. 6 for a forward current $I_F = 30$ mA and the respective input impedance is depicted in Fig. 7. From these results, it can be verified that the LD exhibits a high return loss and impedance mismatch over the range of operating frequencies.

For impedance matching of these circuits, a method for designing nonuniform transmission lines to match complex loads was used [9], although with a heuristic method. The method

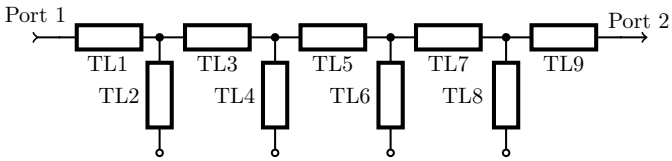

Fig. 8. LD impedance matching circuit with ideal transmission lines.

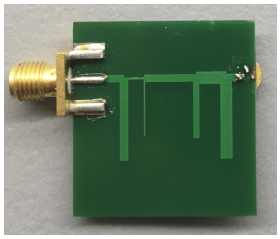

Fig. 9. LD impedance matching circuit PCB.

used made it possible to design nonuniform transmission lines for matching the LD impedance from the S_{11} only. First, a pseudo-low-pass circuit using ideal transmission lines and open stubs, shown in Fig. 8, was numerically optimized over the range of 100 MHz to 2 GHz for an overall S_{11} below -8 dB for the blue LD. From the obtained electrical length and the characteristic impedance (Z_0) of each transmission line, the widths (W) and lengths (L) of the transmission line segments were calculated. These were further optimized using 3D-planar electromagnetic simulator models of the lines based on the frequency-domain method of moments (MoM), to take into account nonideal complex electromagnetic effects such as couplings and parasitics. In Fig. 6 we compare the measured S_{11} through the PCB represented in Fig. 9 against the matched schematic and the electromagnetic simulation. From these results, we see an improvement in the S_{11} which is kept below in the range of $\sim$8 dB.

V. Transmitter Module

As described in Fig. 1, the designed transmitter module includes a current source, a bias-tee, and a temperature control circuit. The latter was based on a proportional-integral (PI) controller to reduce the error between setpoint and current system temperature and, at the output of the PI control loop, two rail-to-rail power amplifiers control the current applied to a TEC, directly attached to the LD mount. This module can stabilize the LD at a constant temperature of 25 °C, provide up to 100 mA DC, and operate with RF frequencies from 100 MHz to 4 GHz. In Fig. 10, the fabricated transmitter module with its individual components is shown, including the impedance matching circuit.

VI. Experimental Results

Firstly, we measured the reflection coefficient of the LD after the impedance matching. In Fig. 6 we can observe a difference in the magnitude between the measured and the simulated reflection coefficient. This difference may be caused by the fact

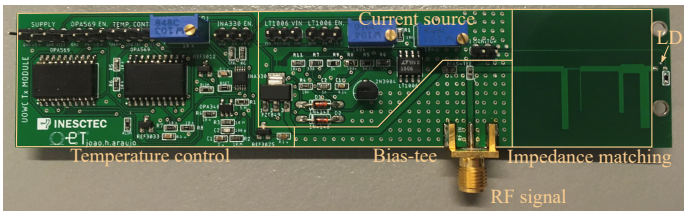

Fig. 10. Designed transmitter module.

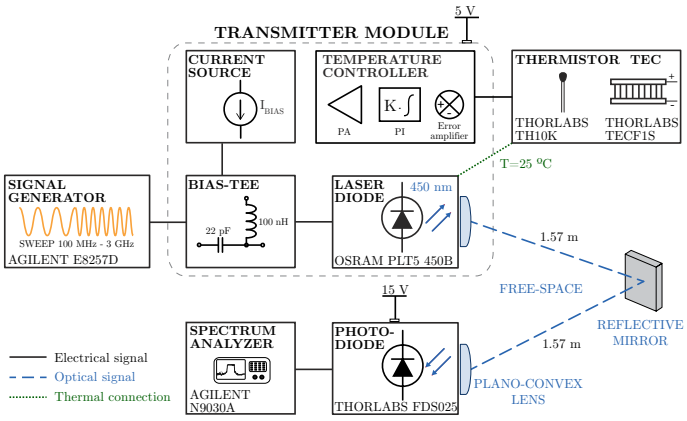

Fig. 11. Frequency response measurement setup.

that the calibration was performed using a standard calibration kit that does not subtract the board inherent effects. However, the frequencies of the obtained maxima (approximately 0.5 GHz and 1.5 GHz) and minima (1 GHz and 1.9 GHz) of magnitude are identical.

To better assess the overall performance of the system, the frequency response was evaluated with and without the impedance matching circuit in free-space following the experimental setup of Fig. 11. The setup includes a signal generator configured to provide a frequency sweep to conveniently modulate the LD. The optical signal is emitted by the LD (with a bias current of 30 mA) in free-space (through the presented transmitter module) with a reflective mirror in the middle of the path over a total distance of 3.14 m. For the receiver side, a high-speed Si photodiode was used. This photodiode has a -3 dB frequency of 7.45 GHz, which would not be the limiting factor of this measurement. Finally, through the spectrum analyzer, it was possible to observe the frequency response shown in Fig. 12. From this result, we see the overall improvement of the system brought by the impedance matching circuit, especially from 600 MHz to 1.6 GHz, with a resonance frequency at 1.5 GHz which is a characteristic of LDs. Above that frequency, we start to observe the referred bandwidth limitation due to the carrier dynamics of the LD, that the matching circuit can not compensate. The roll-off of approximately 6 dB/octave observed at low frequencies is attributed to the LD package parasitics.

In Fig. 13 the received constellation map of an OFDM/16-QAM OWC experimental transmission using the designed module as a transmitter and a high-speed Si photodiode as a

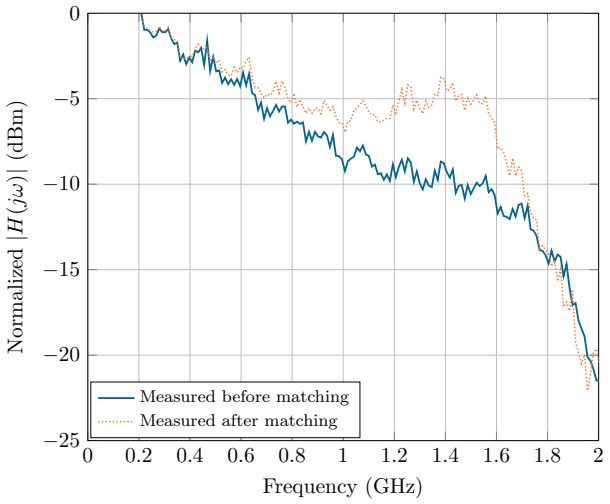

Fig. 12. Normalized frequency response before and after the introduction of the impedance matching circuit for an LD forward current of 30 mA.

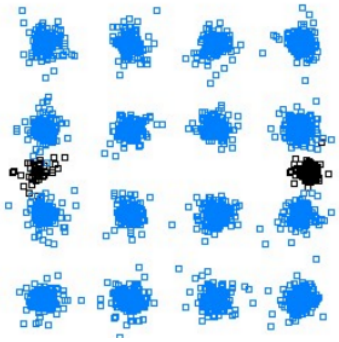

Fig. 13. Received constellation map for a 1.5 GHz signal bandwidth and 4.02 Gbit/s bit-rate OFDM/16-QAM OWC transmission.

receiver is depicted. In the experiment, it was considered a pseudo-random binary sequence composed of 256 subcarriers and an OFDM signal bandwidth of 1.5 GHz, which would allow a bit rate of up to 4.02 Gbit/s. At this bandwidth, with the introduction of the impedance matching circuit we managed to achieve an increased received error vector magnitude (EVM) from −18.33 dB to −22.34 dB, hence a 4 dB EVM improvement.

VII. Conclusion

The design and characterization of an LD based optical wireless communications transmitter module has been discussed in this paper. The proposed system includes a non-uniform transmission line impedance matching circuit which provides a performance improvement of 1 GHz over the 6 dB bandwidth limit. The transmission of a 1.5 GHz bandwidth OFDM signal was demonstrated, where data was mapped into 16-QAM symbols and the corresponding constellation obtained, which proves the suitability of the transmitter for visible light communications, namely underwater optical communications.

References

[1] M. Z. Chowdhury, M. T. Hossan, A. Islam, and Y. M. Jang, "A comparative survey of optical wireless technologies: Architectures and applications," *IEEE Access*, vol. 6, pp. 9819–9840, 2018.

[2] G. Schirripa Spagnolo, L. Cozzella, and F. Leccese, "Underwater optical wireless communications: Overview," *Sensors*, vol. 20, no. 8, p. 2261, Apr 2020.

[3] J. P. Dunsmore, *Handbook of Microwave Component Measurements : with advanced VNA techniques*. John Wiley & Sons, Ltd, 2012.

[4] R. N. Simons, *Coplanar Waveguide Circuits, Components, and Systems*. John Wiley & Sons, Ltd, 2002, ch. 3, pp. 87–111.

[5] D. M. Pozar, *Microwave Engineering*, 4th ed. John Wiley & Sons, Inc., 2011.

[6] C. Mobley, *Light and Water: Radiative Transfer in Natural Waters*. San Diego: Academic Press, 1994.

[7] Y. Q. Wei, J. S. Gustavsson, Å. Haglund, P. Modh, M. Sadeghi, S. M. Wang, and A. Larsson, "High-frequency modulation and bandwidth limitations of gainnas double-quantum-well lasers," *Applied Physics Letters*, vol. 88, no. 5, p. 051103, 2006.

[8] R. Nagarajan and J. E. Bowers, "High-speed lasers," in *Semiconductor Lasers I*, ser. Optics and Photonics, E. Kapon, Ed. San Diego: Academic Press, 1999, pp. 177 – 290.

[9] Gaobiao Xiao and K. Yashiro, "Impedance matching for complex loads through nonuniform transmission lines," *IEEE Transactions on Microwave Theory and Techniques*, vol. 50, no. 6, pp. 1520–1525, 2002.